In Vivo Fluorescence Retinal Imaging Following AAV2-Mediated Gene Delivery in the Rat Retina

Joo Yong Lee,[1] Yoonha Hwang,[2,3] Ji Hyun Kim,[4,5] Yu Sun Kim,[1] Bok Kyoung Jung,[1] Pilhan Kim,[2,3] and Heuiran Lee[4,5]

[1]Department of Ophthalmology, Asan Medical Center, University of Ulsan, College of Medicine, Seoul, Korea
[2]Graduate School of Nanoscience and Technology, Korea Advanced Institute of Science and Technology, Daejeon, Korea
[3]KI for Health Science and Technology, Korea Advanced Institute of Science and Technology, Daejeon, Korea
[4]Department of Microbiology, University of Ulsan, College of Medicine, Seoul, Korea
[5]Cellular Dysfunction Research Center, University of Ulsan, College of Medicine, Seoul, Korea

Correspondence: Heuiran Lee, Department of Microbiology, Cellular Dysfunction Research Center, Asan Medical Center, University of Ulsan, College of Medicine, 88 Olympic-ro 43 Gil Sonpa-gu, Seoul 05505, Republic of Korea;
heuiran@amc.seoul.kr.
Pilhan Kim, Graduate School of Nanoscience and Technology, Korea Advanced Institute of Science and Technology, 291 Daehak-ro, Yuseong, Daejeon 34141, Republic of Korea;
pilhan.kim@kaist.ac.kr.

JYL and YH contributed equally to the work presented here and should therefore be regarded as equivalent authors.

PURPOSE. The purpose of this study was to evaluate longitudinal gene expression patterns by retinal imaging using a modified custom-built confocal laser-scanning microscope in experimental rats after intravitreal injection of recombinant adeno-associated virus 2 (rAAV2-green fluorescent protein [GFP]).

METHODS. Ten 9-week-old Wistar rats were divided into two groups: experimental group (group 1) that received a rAAV2-GFP intravitreal injection and control group (group 2) that received a vehicle. After anesthesia using a Zoletil intraperitoneal injection, 8 µL rAAV2-GFP in group 1 or vehicle in group 2 was injected intravitreally using a 33-G Hamilton syringe. In vivo fluorescence retinal images were acquired under anesthesia at 2, 4, 6, and 13 days after rAAV or vehicle delivery.

RESULTS. Differences in GFP fluorescence were identified starting from day 2 after the intravitreal injection of rAAV2-GFP in group 1. Between days 4 and 6, the intensity and area of fluorescence in the retina began to increase and peaked at day 13. Based on the pattern of GFP expression, the axon of the nerve fiber layer ganglion cell was identified. In group 2, eyes treated with the vehicle showed a small amount of autofluorescence in a limited area for up to 2 weeks, with no increase in intensity during this period.

CONCLUSIONS. In vivo retinal imaging confirmed gene expression within 2 weeks after the intravitreal injection of rAAV2-GFP. Gene transfer and expression in the rat retina occurs quickly in 2 days and appears to peak within 2 weeks of gene delivery. In vivo retinal imaging may be a useful noninvasive tool to continuously monitor gene expression in the retina over time.

Keywords: gene therapy, image analysis, retina

Retinal imaging has developed rapidly for clinical use in the last few years, and technological advancements have allowed for high-definition and wide-field images beyond the typical field of view. The confocal scanning laser ophthalmoscope (cSLO) system uses laser light instead of a bright flash of light to acquire the retinal image. Confocal imaging scans an object point by point using a focused laser beam and then captures the reflected or fluorescent light through a small confocal pinhole. Scattered light from outside of the focal plane, which can cause blurred images, is reduced by this small confocal aperture. The cSLO system allows the capture of sharp, high-contrast topographic slice images of the object.[1] By using well-established fluorescence probes with cSLO, not only structural but also functional and molecular information can be obtained in vivo. Furthermore, multicolor fluorescence imaging is possible with cSLO by using multiple lasers with different beam wavelengths as excitation sources, which enables visualization of interactions between various types of retinal cells labeled with different fluorophores. In addition, wide-field retinal imaging allows us to identify early changes and disease progression not only in the macular area, but in the entire retina, and to better understand the pathophysiology of many retinal diseases.

Rats and mice have been widely used as experimental animals in ophthalmology. In particular, genetically engineered mice or rats have been successfully generated as experimental models for ocular diseases, such as retinal dystrophy. In addition, several retinal imaging tools for the murine eye have been developed.[2–8] A commercially available retinal imaging microscope was generated from a prototype system with a 4 × 4° field of view and further developed with a wider image view and better image contrast.[9] However, the ophthalmic features of rodents, including size and optical features, compared with human eyes limit the acquisition of high-quality images in these small animals.

Retinal degeneration is characterized by the deterioration and loss of visual function due to progressive loss of retinal cell function. Worldwide, 1 in 2000 individuals are affected by

inherited retinal degenerative disorders.[10] The genetic and phenotypic background is known to contribute to clinical features in inherited retinal disorders. In terms of treatment of inherited retinal diseases with identified gene defects, retinal gene therapy has been introduced as a promising treatment modality. In 2008, three independent research groups launched clinical trials using adeno-associated virus (AAV) to the target RPE65 gene for Leber's congenital amaurosis (LCA). The purpose of these clinical trials was to restore vision in young patients suffering from LCA by replacing the dysfunctional gene with the corresponding functional gene by gene transfer into the retina.[11] In addition, many other preclinical and early phase clinical trials using gene therapy for inherited retinal diseases, such as x-linked retinoschisis and choroideremia, are being actively conducted.[12–17]

Considering the pathophysiology and large number of genes related to retinal degeneration, targeting such genes in retinal degenerative diseases maybe an effective therapeutic approach. Before the concepts from animal experiments are transitioned to clinical trials, however, effective gene expression after gene delivery must be demonstrated. The most commonly used methods of validating gene expression are histologic characterization and immunochemistry using antibodies or protein analysis by Western blotting of extracted retinal proteins, which requires enucleation of the eyes from the experimental animals.

In our current study, we used in vivo retinal fluorescence imaging based on a modified custom-built confocal laser-scanning microscope to examine the short-term pattern of gene expression after intravitreal gene delivery in the rat retina. Relay imaging optics were carefully optimized for in vivo retinal imaging in our rodent model with a wide field of view (∼66°). Our results demonstrated the utility of this imaging technology for measuring gene expression levels using the intensity of GFP fluorescence serially driven over an extended period of time by a rAAV-based gene delivery system without the need for scarifying the experimental animals (2 weeks).

METHODS

In Vivo Imaging

In vivo retinal imaging was performed using a custom-built laser-scanning confocal microscopy system modified for retinal imaging from a previously developed intravital confocal imaging platform (Fig. 1A).[18–20] Continuous-wave laser module at 488 nm was used as an excitation sources for GFP. Raster scanning pattern of excitation laser was generated by a scanner system composed of a rotating polygonal mirror (MC-5; Lincoln Laser, Phoenix, AZ, USA) and a galvanometer based scanning mirror (6230H; Cambridge Technology, Bedford, MA, USA), and then delivered to the back aperture of an imaging lens. A high NA objective lens (PlanApoλ, numerical aperture = 0.75; Nikon, Tokyo, Japan) was used as the imaging lens to provide a wide-angle fluorescence image of retina. Fluorescence emission at 500–550 nm was detected by a multialkali photocathode photomultiplier tube (R9110; Hamamatsu Photonics, Hamamatsu, Shizuoka, Japan). The electric signal was digitized by frame grabber (Solios; Matrox, Dorval, Quebec, Canada) and reconstructed to images with a size of 512×512 pixels per frame in real time.

In vivo retina imaging of the rats was performed under systemic anesthesia and pupil dilation. The rats were sedated with 5% isoflurane and anesthetized by intraperitoneal administration of zolazepam, tiletamine (12.5 mg/kg), and xylazine (7.8 mg/kg). After anesthetization, a drop of Mydrin-P (tropicamide 5 mg/mL and phenylephrine 5 mg/mL; Santen

Pharmaceuticals, Osaka, Japan) was applied to the eye of each rat for mydriasis. The anesthetized rat was then fixed on an articulating base (SL20/M; Thorlabs, Newton, NJ, USA) integrated into a motorized three-dimensional (3D) translational stage (3DMS; Sutter Instrument, Novato, CA, USA), which allowed us to image a wide area of the retina by precisely adjusting the imaging angle and position. Fluorescence images were taken by tilting the angle of the rat in four directions around the optic nerve, and the identical location was verified by the vasculature, which was clearly distinguishable from the autofluorescence of the fundus. After imaging, hypromellose (Hycell solution 2%; Samil Pharm., Seoul, Korea) was applied on the eye to prevent excessive dehydration during recovery.

Recombinant AAV Preparation and Titration

Using a triple-transfection method, self-complementary rAAV-expressing green fluorescent protein (GFP) under a cytomegalovirus (CMV) promoter was produced.[21] For large-scale rAAV preparation, 293T cells were transfected in $20- \times 10$-cm dishes. rAAVs were released and purified from cell lysates using two sequential CsCl gradient steps. After dialysis in 10 mM Tris buffer (pH 7.9) containing 2 mM $MgCl_2$ and 2% sorbitol, rAAVs were aliquoted and stored at $-80°C$. The number of total and infectious rAAV particles was quantified by real-time quantitative PCR targeting the CMV promoter and by monitoring GFP expression in HeLa cells after rAAV-GFP treatment, respectively. We used rAAV2-GFP solution containing 6.27×10^8 infectious particles (IPs) per 1 mL of solution, with a ratio of 361.88 total particles to each infectious particle (Supplementary Fig. S1).

Animal Care and Preparation

Nine-week-old male Wistar rats were used in all experiments. All live rat experiments were approved by the Institutional Animal Care and Use Committee of Asan Medical Center (Seoul, Korea) and the Animal Care Committee of Korea Advanced Institute of Science and Technology (Daejeon, Korea). All animals were treated, maintained, and euthanized in accordance with the policies specified in the ARVO statement for the Use of Animals in Ophthalmic and Vision Research and the guidelines approved by national and local institutions.

Intravitreal Injection

Nine-week-old Wistar rats were anesthetized by intraperitoneal injection of zolazepam and tiletamine (12.5 mg/kg). The intravitreal injection was done using a 33-G Hamilton syringe (Hamilton, Bonaduz, Switzerland) under the operating microscope (Zeiss, Oberkochen, Germany) after dilation of the pupil with Mydrin-P (tropicamide 5 mg/mL and phenylephrine 5 mg/ mL; Santen Pharmaceuticals). A sclerotomy was made approximately 1 mm posterior to the limbus with a 33-G Hamilton syringe, taking caution to avoid damaging the lens. A total of 8 µL rAAV2-GFP (5.02×10^6 IPs) or vehicle was administered intravitreally in the experimental ($n = 5$) or control ($n = 5$) group, respectively (Fig. 1B).

Immunoblot Analysis

ARPE-19 cells, a spontaneously arising RPE cell, were infected with rAAV-GFP, and cells were lysed at designated times. Proteins were resolved on SDS-polyacrylamide gels and then transferred to polyvinylidene fluoride membranes. After blocking with Tris-buffered saline containing 0.1% Tween-20 and 5% (wt/vol) bovine serum albumin (BSA), the membranes
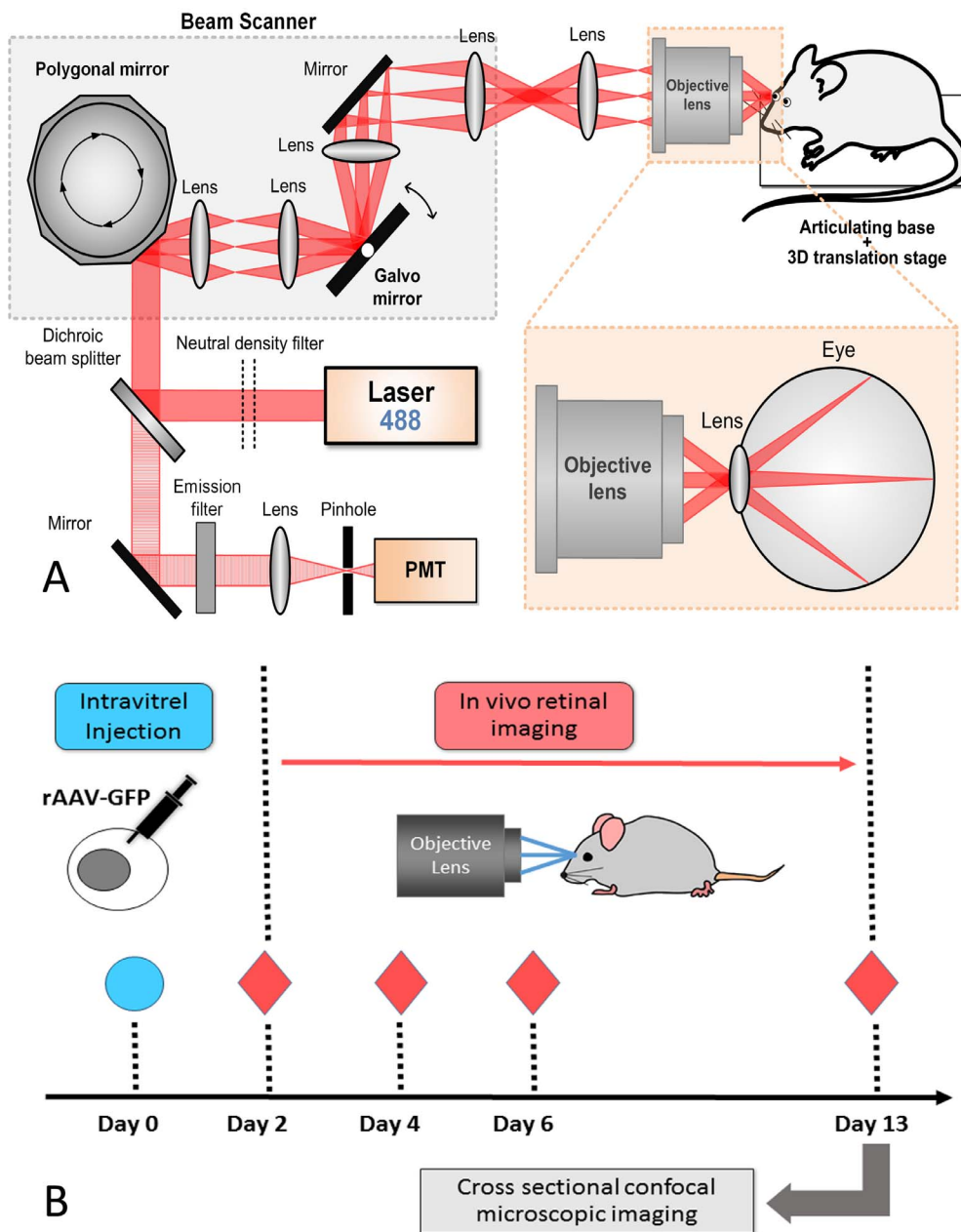
FIGURE 1. (A) Experimental setup of a custom-built laser-scanning confocal microscope. (B) Schema for rAAV2-GFP delivery. After intravitreal rAAV2-GFP injection into the rat, in vivo serial imaging was performed on days 2, 4, 6, and 13. On day 13, one of the rats that received the rAAV2-GFP intravitreal injection underwent cross-sectional confocal microscopic imaging.

were incubated with primary antibodies and appropriate secondary antibodies (Jackson ImmunoResearch Laboratories, West Grove, PA, USA). Bands were detected using an enhanced chemiluminescence system. Green fluorescent protein antibodies were obtained from Invitrogen (Camarillo, CA, USA). β-Actin antibodies were obtained from Sigma (St. Louis, MO, USA).

## Fluorescence Microscopy After Intravitreal Injection

One of the Wistar rats receiving the 8-μL rAAV-GFP intravitreal injection was used for fluorescence microscopy. Under deep anesthesia using zolazepam and tiletamine (12.5 mg/kg), the

eyeball was dissected out and stored at −20°C without fixation. The eyecups were then embedded in an optimum cutting temperature compound and sectioned horizontally at 6 μm thickness using a cryostat microtome (Microm HM550; Thermo Scientific, Waltham, MA, USA). Sections were cut to include the full length of the retina, from the cornea to the posterior pole. Gene-transfected cells were identified by GFP expression under the confocal microscope system (LSM 780; Zeiss).

To identify the specific cell layer in the retina expressing GFP, the frozen retina was stained with 4′,6-diamidino-2-phenylindole (DAPI). Prior to DAPI staining, the tissue was first fixed with cold methanol. Sections were blocked in 10% BSA and stained with DAPI.
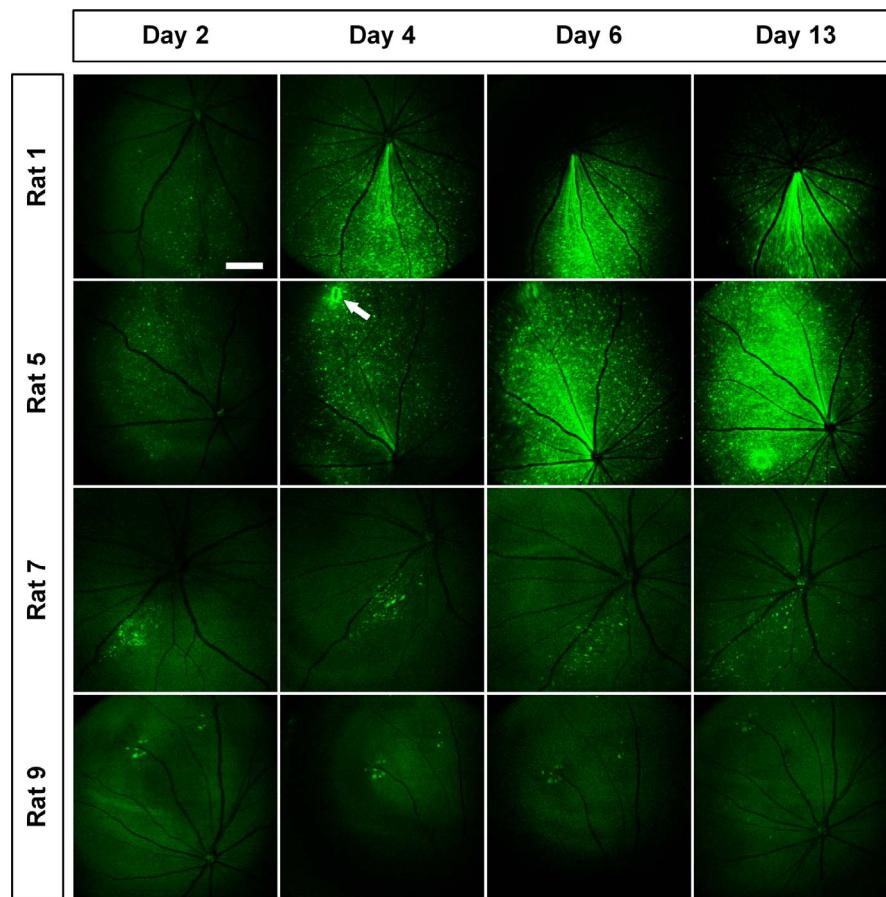
FIGURE 2. In vivo time course of GFP expression in the fundus of rat experimental (rats 1 and 5) and control (rats 7 and 9) groups. In vivo time course of GFP expression in the fundus of rat experimental (rats 1 and 5) and control (rats 7 and 9) groups. The intensity of GFP expression increased over time in rats 1 and 5, and significant GFP expression was noted in all rats after day 4. The GFP intensity seemed to reach a maximal level on day 13. In rat 5, a hyperfluorescent spot (_white arrow_) in the superior area was caused by GFP gene delivery at the injection site. In contrast, in rats 7 and 9, hyperfluorescent spots were identified only in a limited area from day 2 or 4, and the intensity and area of hyperfluorescence remained at a similar level until day 13 (_Scale bar_: 1 mm).

RESULTS

### In Vivo Imaging Using Custom-Built Laser-Scanning Confocal Microscopy

In the experimental group that received an intravitreal injection of rAAV2-GFP, weak GFP fluorescence signals in the treated retina were noted from day 2 (Supplementary Fig. S2), and the fluorescence intensity consistently increased during the experimental period (Fig. 2). There was no green fluorescence signal in the untreated retinas (data not shown). The nerve fiber layer (axon of ganglion cell) could be seen, and the extent and intensity of the fluorescence signal in the nerve fiber layer also increased during the time course (Fig. 2), with a peak in intensity detected on day 13. Based on our pilot study, the level of GFP expression was similar between weeks 2 and 3 (data not shown), indicating that the level of GFP expression likely peaks at week 2. Even with careful intravitreal injection procedure, traumatic cataracts occurred in rats 3 and 4. Due to lens opacity, fluorescence could be partially seen only in the middle of the retinal image from day 2. In addition, in rat 5, increased fluorescence was seen in the upper area on day 4, with a hyperfluorescent spot at the injection site caused by the 33-G needle.

In the control group, retinal imaging showed different levels of fluorescence in different animals (Supplementary Fig. S3). In rat 6, no hyperfluorescent spots were identified until day 13. In four rats (7–10), hyperfluorescent spots were identified in a limited area from day 2 or 4, and the intensity and area of hyperfluorescence remained constant during the experimental period (Fig. 2). Generally, the intensity and extent of GFP expression did not significantly change during the time course. In contrast to the experimental group, the nerve fiber layer could not be visualized during the time course in the control group.

To examine the persistence of GFP expression over time following gene transfer by rAAV2 in vitro, ARPE-19 cells were transduced with rAAV2-GFP and maintained for 14 days by subculturing whenever necessary (Fig. 3). A GFP signal was clearly observed 2 days after virus administration and was retained for the entire experimental period (Fig. 3A). As expected, GFP expression was also readily detected by Western blotting analysis, with no substantial change in the degree of GFP expression (Fig. 3B).

### Cross-Sectional Image of Fluorescence Microscopy

Based on our serial in vivo retinal images, we speculated that intravitreal rAAV2-GFP injection may only affect the inner
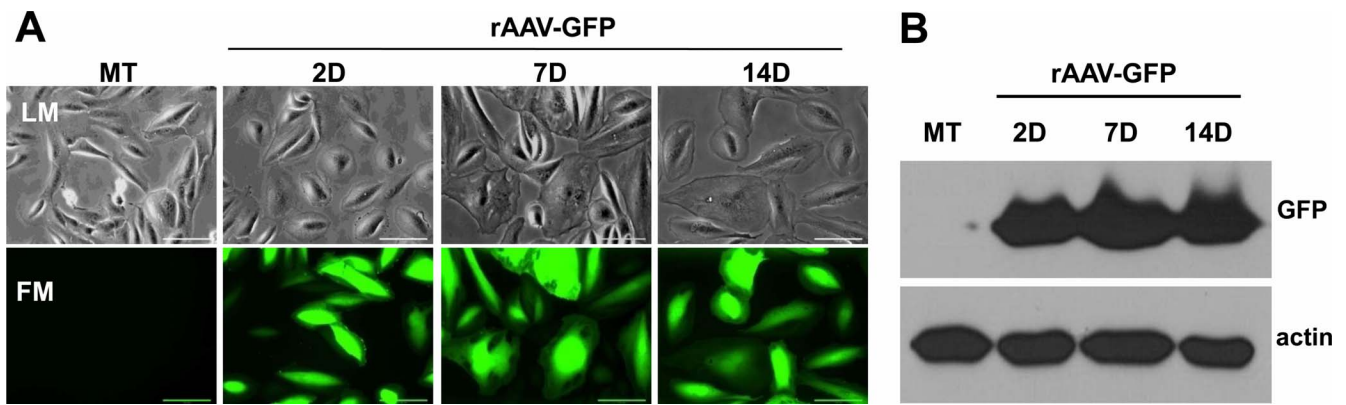
FIGURE 3. (A) The characteristics of GFP expression in ARPE-19 cells. Cells were transduced with rAAV2-GFP at 1×10^4 multiplicity of infection, and the cells were maintained for 14 days. At designated time points, GFP expression was readily visualized by examining the cells using fluorescence microscopy. (B) Western blotting of cell lysates was also carried out to quantify the degree of GFP expression. The data show significant expression of rAAV2-delivered GFP for 14 days in ARPE cells. LM, light microscopy; FM, fluorescence microscopy (*Scale bar*: 100 μm).

retinal cell layers, such as retinal ganglion cells. After visualization of the cell body from day 2 or 4, the nerve fiber layer and axons of ganglion cells were detectable as of day 4 and until day 13. Confocal images of the horizontal cross-sectional view also revealed GFP expression in the ganglion cell layer, inner plexiform layer, and outer nuclear layer. However, using DAPI staining, GFP expression was not identified in the inner or outer nuclear layers (Fig. 4).
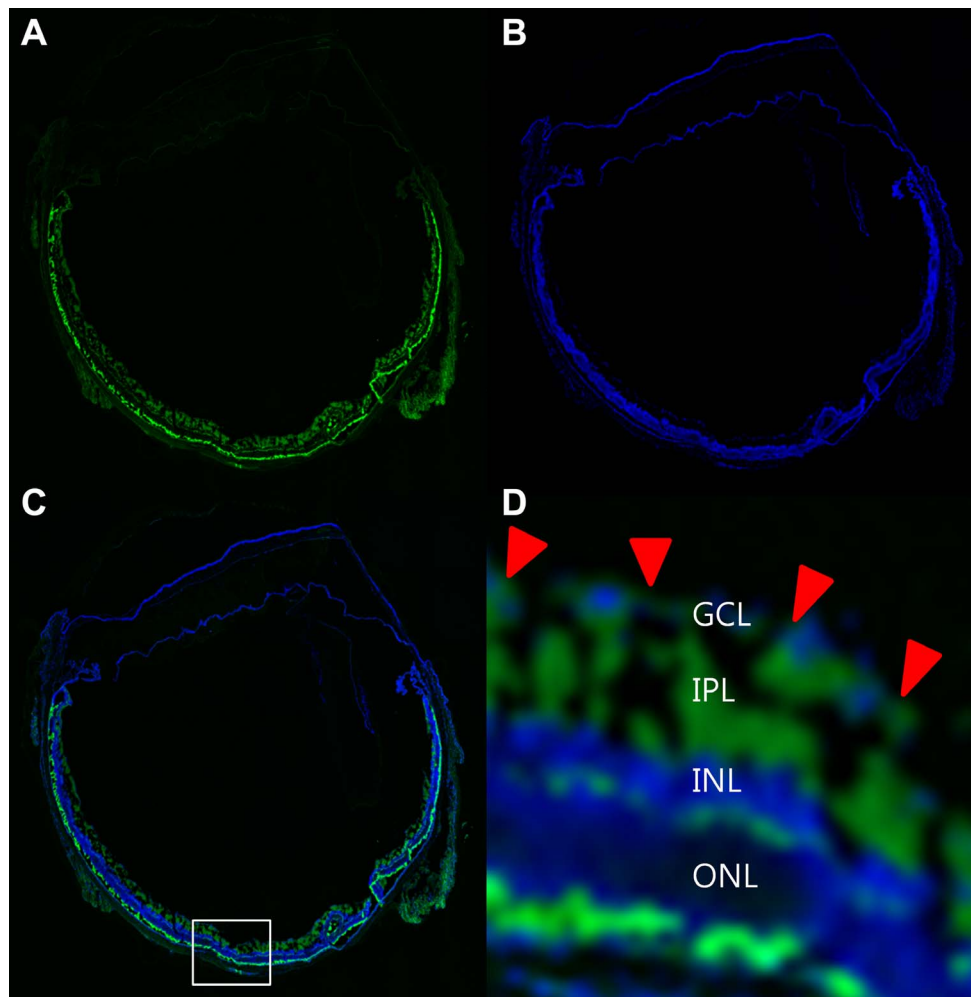
FIGURE 4. Whole eye confocal cross-sectional retinal images on day 13. (A) Cross-sectional image showing GFP expression. (B) Same confocal image as in A stained with DAPI. (C) Merged GFP and DAPI images. (D) High-magnification image of *boxed area* in C. *Arrowheads* mark double + cells in GCL. GCL, ganglion cell layer; IPL, inner plexiform layer; INL, inner nuclear layer; ONL, outer nuclear layer.

Investigative Ophthalmology & Visual Science

Discussion

Our present study findings showed that in vivo retinal imaging in a rat using a modified custom-built confocal laser-scanning microscope after intravitreal gene transfer can be used as a longitudinal monitoring method for assessing gene expression. Based on high-quality serial images, changes in gene expression in the retina of each animal could be visualized over time. In addition, the field of view of each image included the optic disc and almost the entire posterior pole of the rat retina, which allowed us to evaluate the overall changes in the retina of the experimental rat group. Considering the noninvasive nature of this technique, fluorescence retinal imaging may provide us valuable information on the long-term natural course of genetic expression in transgenic or gene-treated rodents.

Retinal imaging tools to capture color fundus photography and fluorescence angiography images in experimental rodents are already available.[9] However, in vivo fluorescence retinal imaging of gene-transfected or transgenic rodents remains challenging for several reasons, such as reduced image resolution by wavefront aberration induced by the rodent eye and poor signal-to-noise ratio from thermal and shot noise of the detector and its amplifier. To improve image quality, image averaging methods, rather than improvements in the optical system, have been previously investigated and could enhance cellular resolution to a limited extent.[22] In our present study, by utilizing high NA objective lens, optimally matched relay lens optics, a high-sensitivity photomultiplier tubes (PMT) detector, and a 488-nm laser excitation source, which were integrated into a custom-built confocal microscopy platform, we successfully acquired high-quality retinal images of GFP expression, which were sufficient for evaluation of gene expression.

Moreover, our system provided us a wider field of fundus image, up to 66° in the rat eyes, which is much wider than that acquired by the current commercially available fundus cameras for animal experiments. These findings suggest that the fundus image obtained by our current technique can provide comprehensive information on gene expression from the entire retina following gene transfer. As a result, montage image preparation to show the entire retina is not necessary. One of the main disadvantages of a montage image is that the quality can vary between images. With wide retinal image data, we can readily acquire reliable data, such as changes in intensity level of fluorescence expression over time and the movement of fluorescence from cell to cell or in the intracellular structure in the whole retina. Serial images also show the pattern of progression of gene expression over time. To avoid iatrogenic lens and retinal trauma, the needle tip was located just near the injection site shallowly during the intravitreal injection. Yet, the area of gene expression reached almost the entire retinal area at day 13 from only a limited area at day 2 or 4. These results suggest that circulation in the vitreous itself or cell-to-cell communication between the retinal cells can be viewed using gene transfer.

In the control group, which received only an injection of vehicle, fluorescence was observed in a limited area around the retinal puncture site after day 2 or 4, depending on the subject. The fact that the contralateral eyes with no intraocular injection did not show any fluorescence during the time course suggests that mechanical trauma in the retina may contribute to the development of autofluorescence. The autofluorescence induced by mechanical trauma is distinguishable from real GFP expression after gene transfer, however, because the latter shows increasing intensity and expansion of the area of fluorescence. In the experimental group, the nerve fiber layer was visualized after GFP expression in the retinal ganglion cell body from day 4. However, in the control group, the autofluorescence pattern remained relatively stable without an increase in intensity or extent, and no nerve fiber layer visualization was noted in any control animal. These findings may be useful to differentiate between true expression of the transferred gene and autofluorescence. Collectively, serial in vivo retinal images in the same subject, as done in the present study, is crucial for gene expression analysis.

If more reliable and reproducible image processing techniques were available, the intensity of fluorescence could be quantified, and such numerical data could be used to quantify specific protein expression level following gene transfection into the cells. If we could identify a significant correlation between the imaging analysis and protein expression level, this imaging tool could be used as a noninvasive indirect pharmacokinetic analysis method. Previous studies have attempted to acquire functional images using similar concepts. Yin et al.[3] acquired functional images of individual mouse retinal ganglion cells using a genetically encoded calcium indicator. One of the great advantages of these functional imaging techniques is that they allow repeated imaging of cells or tissues while avoiding damage to the eye. Such functional imaging would have various applications, such as identification of dose levels of administered intraocular drugs in phase I clinical trials, and pharmacokinetic/dynamic analysis. In contrast to other organs, acquiring specimens from the vitreous and retina requires an invasive procedure which cannot be repeated in a short-time period. Therefore, noninvasive methods of analyzing the pharmacokinetic profile may be valuable in the development of new intraocular drugs.

In our present analyses, only intravitreal injection was performed. However, subretinal injection is another common method to introduce a gene into the eye in animal experiments. Depending on the retinal disease, such as photoreceptor degeneration and chorioretinal neovascularization, subretinal injection may be more effective. As shown in the confocal cross-sectional image (Fig. 4), GFP expression was seen only in the ganglion cell layer and not in the photoreceptor cell layer, even on day 13, the day of maximal GFP expression based on in vivo imaging. Considering these findings, even though subretinal injection may be a more invasive method to deliver gene therapy into the eye, it may be appropriate when aiming for the outer retina.

In conclusion, in vivo retinal imaging in rats confirmed the pattern of gene expression within 2 weeks of the intravitreal injection of rAAV2. Gene transfer and expression in the rat retina takes place quickly and seems to reach a peak level within 2 weeks of gene delivery. In vivo retinal imaging in this system may be a noninvasive and very useful approach to monitoring gene expression in the retina over time.

References

1. Sharp PF, Manivannan A. The scanning laser ophthalmoscope. *Phys Med Biol*. 1997;42:951–966.

2. Geng Y, Greenberg KP, Wolfe R, et al. In vivo imaging of microscopic structures in the rat retina. *Invest Ophthalmol Vis Sci*. 2009;50:5872–5879.

3. Yin L, Geng Y, Osakada F, et al. Imaging light responses of retinal ganglion cells in the living mouse eye. *J Neurophysiol*. 2013;109:2415–2421.

4. Palczewska G, Dong Z, Golczak M, et al. Noninvasive two-photon microscopy imaging of mouse retina and retinal pigment epithelium through the pupil of the eye. *Nat Med*. 2014;20:785–789.

5. Zhang P, Zam A, Pugh EN, Zawadzki RJ. Evaluation of state-of-the-art imaging systems for in vivo monitoring of retinal structure in mice: current capabilities and limitations. In: *Proceedings of SPIE 8930, Ophthalmic Technologies XXIV*;2014:893005.

6. Stremplewski P, Komar K, Palczewski K, Wojtkowski M, Palczewska G. Periscope for noninvasive two-photon imaging of murine retina in vivo. *Biomed Opt Express*. 2015;6:3352–3361.

7. Zhang P, Zam A, Jian Y, et al. In vivo wide-field multispectral scanning laser ophthalmoscopy-optical coherence tomography mouse retinal imager: longitudinal imaging of ganglion cells, microglia, and Müller glia, and mapping of the mouse retinal and choroidal vasculature. *J Biomed Opt*. 2015;20:126005.

8. Bar-Noam AS, Farah N, Shoham S. Correction-free remotely scanned two-photon in vivo mouse retinal imaging. *Light Sci Appl*. 2016;5:e16007.

9. Phoenix micron IV retinal imaging microscope. Phoenix Research Labs. Available at: http://www.phoenixreslabs.com/products/micron-iv-retinal-imaging-microscope. Accessed June 15, 2016.

10. Sohocki MM, Daiger SP, Bowne SJ, et al. Prevalence of mutations causing retinitis pigmentosa and other inherited retinopathies. *Hum Mutat*. 2001;17:42–51.

11. Maguire AM, Simonelli F, Pierce EA, et al. Safety and efficacy of gene transfer for Leber's congenital amaurosis. *N Engl J Med*. 2008;358:2240–2248.

12. Ou J, Vijayasarathy C, Ziccardi L, et al. Synaptic pathology and therapeutic repair in adult retinoschisis mouse by AAV-RS1 transfer. *J Clin Invest*. 2015;125:2891–2903.

13. Zeng Y, Takada Y, Kjellstrom S, et al. RS-1 gene delivery to an adult Rs1h knockout mouse model restores ERG b-Wave with reversal of the electronegative waveform of X-linked retinoschisis. *Invest Ophthalmol Vis Sci*. 2004;45:3279–3285.

14. Takada Y, Vijayasarathy C, Zeng Y, Kjellstrom S, Bush RA, Sieving PA. Synaptic pathology in retinoschisis knockout (Rs1-/y) mouse retina and modification by rAAV-Rs1 gene delivery. *Invest Ophthalmol Vis Sci*. 2008;49:3677–3686.

15. Vasireddy V, Mills JA, Gaddameedi R, et al. AAV-mediated gene therapy for choroideremia: preclinical studies in personalized models. *PLoS One*. 2013;8:e61396.

16. Zein WM, Jeffrey BG, Wiley HE, et al. CNGB3-achromatopsia clinical trial with CNTF: diminished rod pathway responses with no evidence of improvement in cone function. *Invest Ophthalmol Vis Sci*. 2014;55:6301–6308.

17. Marangoni D, Vijayasarathy C, Bush RA, Wei LL, Wen R, Sieving PA. Intravitreal ciliary neurotrophic factor transiently improves cone-mediated function in a CNGB3$^{-/-}$ mouse model of achromatopsia. *Invest Ophthalmol Vis Sci*. 2015;56:6810–6822.

18. Hwang Y, Ahn J, Mun J, et al. In vivo analysis of THz wave irradiation induced acute inflammatory response in skin by laser-scanning confocal microscopy. *Opt Express*. 2014;22:11465–11475.

19. Ahn J, Choe K, Wang T, et al. In vivo longitudinal cellular imaging of small intestine by side-view endomicroscopy. *Biomed Opt Express*. 2015;6:3963–3972.

20. Choe K, Jang JY, Park I, et al. Intravital imaging of intestinal lacteals unveils lipid drainage through contractility. *J Clin Invest*. 2015;125:4042–4052.

21. Kim SJ, Lee WI, Heo H, Shin O, Kwon YK, Lee H. Stable gene expression by self-complementary adeno-associated viruses in human MSCs. *Biochem Biophys Res Commun*. 2007;360:573–579.

22. Kumar S, Ho G, Woo KM, Zhuo L. Achieving cellular resolution for in vivo retinal images of transgenic GFAP-GFP mice via image processing. *Opt Express*. 2008;16:8250–8262.

Investigative Ophthalmology & Visual Science